

Journal of Biomedical Optics

SPIEDigitalLibrary.org/jbo

Comparative study of the angle-resolved backscattering properties of collagen fibers in bovine tendon and cartilage

Deepa K. Kasaragod
Zenghai Lu
Stephen J. Matcher



Comparative study of the angle-resolved backscattering properties of collagen fibers in bovine tendon and cartilage

Deepa K. Kasaragod, Zenghai Lu, and Stephen J. Matcher

University of Sheffield, Department of Material Sciences and Engineering, Kroto Research Institute, North Campus, Broad Lane, Sheffield, S37HQ, United Kingdom

Abstract. In a biological tissue, light scattering is based on the size and type of scatterers seen as refractive index variations that describe the optical properties shown. In this paper, we have implemented the variable incidence angle technique of multiple angle of illumination experiment on tendon and cartilage samples whose dominant constituents are genetically different types of collagen fibers, type I and type II, respectively. It is found that tendon displays a much greater angular anisotropy in its optical backscattering coefficient than the healthy cartilage. We propose that this is due to a more uniform distribution of fine fibrils than is found in tendon. Rayleigh–Gans approximation is used to give qualitative support to this idea. © 2011 Society of Photo-Optical Instrumentation Engineers (SPIE). [DOI: 10.1117/1.3606564]

Keywords: cartilage; tendon; type I collagen; type II collagen; optical coherence tomography; angle-resolved backscattering; Rayleigh–Gans scattering.

Paper 11164LR received Apr. 5, 2011; revised manuscript received Jun. 9, 2011; accepted for publication Jun. 10, 2011; published online Aug. 5, 2011.

Optical coherence tomography (OCT) has long been established as a noninvasive imaging tool to study the structural profile of the biological tissues.¹ Polarization-sensitive OCT (PS-OCT) studies have been carried out on cartilage by various research groups, based on the birefringent property of the optical anisotropic collagen fiber forming the articular cartilage.^{2,3} A multiple angle of illumination study called variable incidence angle experiment, along with polarimetric analysis, has been applied to study the optical anisotropic characteristics shown by biological tissue such as cartilage.^{3,4}

Collagen fibers form the major constituent of the connective tissue of the human body. The study of scattering properties of the light incident on the biological tissues is a signature of the type of scatterers present in the specimen.⁵ More details on quantitative studies on polarized light interaction in tissues is given here.⁶ It has been demonstrated that angle-resolved backscatter can accurately size the spherical scatterers, with applications, e.g., in detecting abnormal cell nuclei as reported by Wax et al.⁷

The nature of the optical backscattering differences between different types of collagen molecules arise due to the difference in the underlying molecular organization: Type I collagen fibers in tendon and Type II collagen fibers in articular cartilage.⁸

In this paper, we present a comparative study of the optical backscattering properties obtained using an OCT system over different angles of illumination, of the different scatterers type involved in the collagen fiber networks of bovine tendon and cartilage samples. Backscattering profiles obtained from the angle-resolved experiment has been interpreted using Rayleigh–Gans (RG) scattering approximation, upon treating the collagen fibril as a finite cylinder.

Fresh bovine cartilage samples were extracted from the fetlock joint of the hind limb and deep-frozen until required. Tendon samples found along this section of the hind limb were also extracted. The experiments were carried out on the anterior side of the apex of the cartilage, within 24 h of extracting the sample. Tendon samples were sectioned along the macroscopically visible collagen fiber direction. The OCT system used for this study is a swept source-based continuous polarization modulation PS-OCT system. For this study, we only use the obtained reflectivity data. A detailed description of the system is given elsewhere.⁹ In the PS-OCT system, the optical signals are obtained in two orthogonally polarized optical channels. The two components, a_h and a_v , represent the moduli of the complex A-scans (obtained by fast Fourier transform of the obtained swept source interferogram) in the horizontally and vertically polarized channels as obtained in the two balanced photoreceivers. These two signals are combined to represent the optical reflectivity profiles expressed in decibels.

$$R_{\text{dB}}(z) = 10 \log_{10}[a_h(z)^2 + a_v(z)^2]. \quad (1)$$

This depth dependent plot obtained upon averaging over 50 lateral A-scans is fitted linearly. The y-intercept of the linear fit is taken to be directly proportional to the optical backscattering coefficient. The optical backscattering is thus obtained for different angle of incident light illumination ranging from +40 to –40 deg with a step of 20 deg for tendon and cartilage samples in two orthogonal planes of imaging [Fig. 1]. Typical depth-dependent optical reflectivity profiles in decibels obtained for the tendon and cartilage over 50 A-scan averages are shown in Figs. 2(a) and 2(b).

It is immediately apparent that the single backscatter approximation is only valid for the lower region of the cartilage depth profile as the gradient of reflectivity versus depth is positive in the upper region [Fig. 2(b)]. Interestingly, this is similar to the results seen in some dysplastic oral tissues.¹⁰ Such behavior can be explained by a depth dependent increase in the backscatter coefficient whose magnitude more than compensates for the decrease in the beam intensity due to elastic scatter. This could arise through changes in cell or fiber density, size, alignment, or changes in tissue refractive indices. In the following analysis we consider the regression intercept separately for both the cartilage regions and plot each as a function of the angle. For the tendon, the single-scatter relationship appears to hold and so the distinction need not be made.

Scattering from the microstructures in biological tissues often fall within the RG scattering approximation regime. RG theory is

Address all correspondence to: Deepa Kasaragod, University of Sheffield, Materials Science and Engineering, Broad Lane, Sheffield, South Yorkshire s3 7HQ United Kingdom; Tel: 07824487940; E-mail: mtp08dk@sheffield.ac.uk.

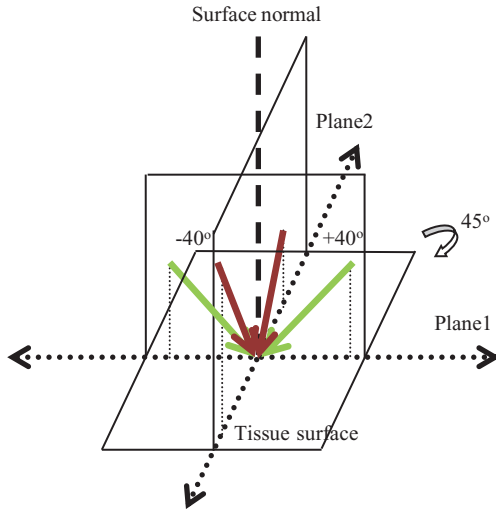


Fig. 1 Schematic of the experimental procedure followed for imaging the tissue in two orthogonal planes and multiple angles of incidence. For cartilage tissue sample, the plane of azimuth is rotated to 45 deg and then the similar set of experiment was carried out in the rotated planes.

equivalent to the first order Born approximation scattering theory of quantum mechanics, where the intraparticle multiple scattering has been disregarded by assuming unperturbed light field interaction of small polarizability.¹¹ In our studies, collagen fibril has been modeled as a finite cylinder of length $2L$ and diameter $2a$ and the backscattered intensity of light has been simulated over a scattering volume V , and the angle-resolved scattered light intensity in decibels are obtained for different geometry of scatterers involved in tendon and cartilage, according to the equation for total scattered field from finite cylinder given in Ref. 11.

The plots of the optical backscattering coefficients over multiple angles of illumination for two different orthogonal planes of imaging for bovine tendon and cartilage samples are as shown

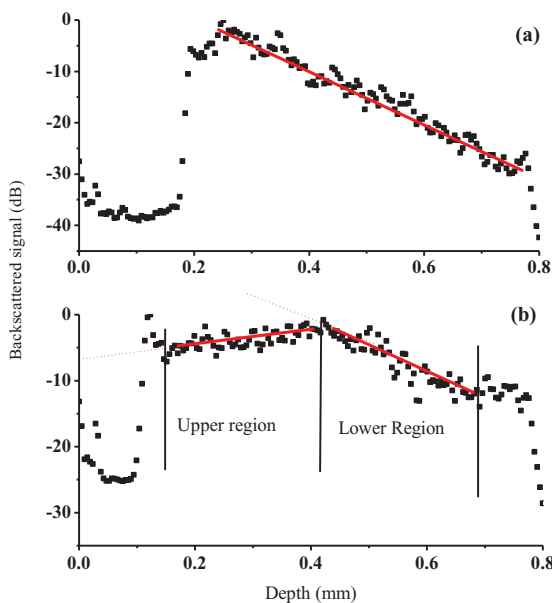


Fig. 2 (a) Representation of the reflectivity profile fitted to a linear curve and extrapolated to intercept the y-axis to obtain the backscattering coefficient for tendon and (b) cartilage.

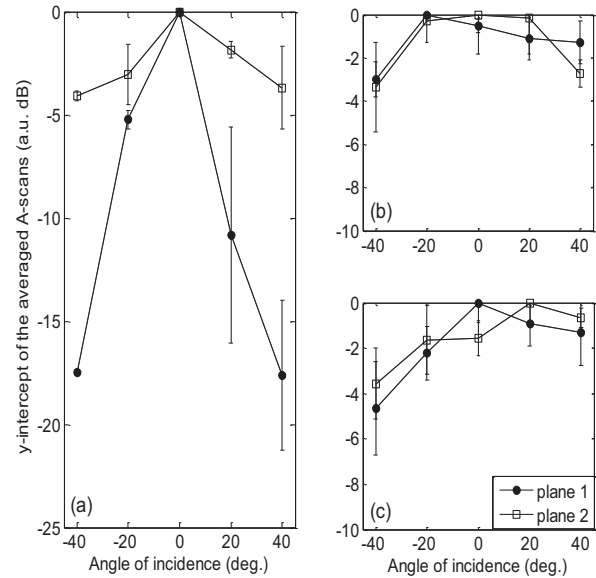


Fig. 3 Curves of y-intercepts of averaged A-scans obtained for different angle of light illumination in two different orthogonal planes for (a) tendon and (b) cartilage upper region. (c) Cartilage lower region as in Fig. 2(b).

in Figs. 3(a)–3(c). Figure 3(b) is obtained from the upper region of the reflectivity profile fit as is seen from Fig. 2(b) and likewise for Fig. 3(c), which gives the latter half of the reflectivity profile fit. The error bars represent the standard deviation over three repeats for both tendon and cartilage. For the tendon, the two orthogonal planes are chosen to be the $x-z$ and $y-z$ planes, the Cartesian coordinate system is chosen such that the collagen fibers are aligned along the x -direction and the axial depth is along the z -direction. For cartilage, it is not possible to visualize by eye the collagen fiber direction and hence, not possible to establish a coordinate system in this manner. Instead, the x, y axes are defined relative to the anatomical planes of the joint. The fetlock joint constrains the two connected bones to flex within the “sagittal” plane and this plane then is defined as $x-z$. We refer to this set of coordinates as the sagittal system. Of course, a problem arises if the angle-resolved variations in backscatter occur predominately when the beam is inclined in a plane containing the fiber axis, then the unknown orientation of cartilage collagen fibrils relative to this sagittal system lead to a potential ambiguity. In particular, if the fibrils happen to be oriented at 45 deg of azimuth (i.e., rotation about z -axis) relative to the sagittal plane, then by symmetry, no differences would occur between two sets of measurements in the two planes. To try to address this, we supplement measurements taken relative to the sagittal system with measurements taken relative to a system that is rotated azimuthally through 45 deg. If fibrils are oriented as described, then the first set of measurements would show a negligible effect, whereas the second set would show a maximal effect. The scattering profiles of cartilage measured using these two coordinate systems are found to agree to within the error bars shown in Figs. 3(b) and 3(c).

The fall in the backscattered optical signal from normal to oblique incidence of 40 deg falls in the range 0.5 to 4 dB for the cartilage sample, whereas the signal drop is remarkably high (~ 17 to 18 dB) in the case of the tendon sample. This reflects the basic difference in the scattering nature involved with the

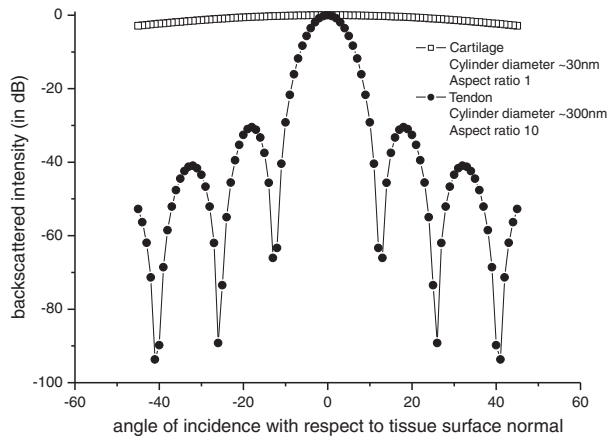


Fig. 4 The angle-resolved back-scattered intensity profiles in decibels obtained from implementation of scattering simulation using Rayleigh-Gans approximation for single fibril cylinder of cartilage (diameter ~ 30 nm) of aspect ratio unity and tendon (diameter ~ 300 nm) fibril of aspect ratio 10. Note how the physically anisotropic structures (increased cylinder aspect ratio) are associated with a more rapid fall in backscatter with respect to the scattering angle.

two types of tissues. The scattering plots obtained for cartilage samples represents isotropic scattering event and the profile obtained for multiple illumination angles is similar over four planes of imaging oriented at 45 deg of azimuth relative to each other. In the tendon sample, the differences in the backscattering profiles obtained over two orthogonal planes differ over almost 18 dB. Preliminary studies carried out by evaluating the backscatter coefficient of a finite cylinder of given radius and aspect ratio to model the two different tissues using RG approximation provides a possible explanation to this difference in the angle-resolved backscattering obtained in Fig. 4. The hypothesis is that the finer and smaller diameter (~ 30 nm) collagen fibrils in cartilage tend to show a more isotropic behavior as if the scatterer involved is a homogeneous cylinder of aspect ratio unity. The tendon fibrils show a more anisotropic behavior owing to the wavy-like (crimp structure) and the larger diameter fibrils involved. Also, referring to the random size distribution of fibrils as given by Freund et al.,¹² we speculate that the effective scattering behavior shown by the coarse packing nature of large fibrils separated by smaller fibrils in tendon tissue tend to be more anisotropic as would be dominated by behavior similar to larger size and higher aspect ratio cylinders [~ 10 as in Fig. 4]. A much more rigorous analysis can be carried out by taking into account the packing density of the collagen fibers and the three-dimensional arrangements of scatterers involved in both tendon¹² and cartilage over a scattering volume, as determined by the lateral and axial resolution of the PS-OCT system used for imaging. Such a model would potentially reproduce the observed features of the angle-resolved backscatter, while features that are not observed (e.g., the periodic oscillations in backscatter with respect to angle) would possibly be suppressed by averaging over an ensemble of fibers within the focal spot with a distribution of radii,¹² as well as averaging over a range of angles defined by the beam numerical aperture (about 2 deg). This is currently ongoing in our group and the results will be reported in due course.

The measurement of angle-resolved backscatter has generated considerable interest when applied to cells as it offers the

potential to estimate the size of spherical scatterers such as the cell nuclei.⁷ Our study has been to extend this approach to wide angles of optical backscattering from fibrous connective tissues containing collagen fibers of different size and to demonstrate significant differences between scattering profiles of bovine tendon and cartilage. We hypothesize that the differences in the angle-resolved backscattering profiles arise due to differences in the collagen fiber diameter and packing arrangement. This could potentially lead to diagnostic applications as in, for example, osteoarthritis lesion development there is often a replacement of native type II hyaline cartilage with more fibrous type I collagen-based repair tissue, which is found to possess inadequate mechanical properties to successfully replace the original tissue. Further studies have to be carried out to provide complete insight into potential application of angle-resolved backscatter to study connective tissues.

The authors would like to thank Dr. A. Crawford and Dr. R. Goodchild, School of Dentistry, University of Sheffield toward the help provided in collecting and dissecting the bovine cartilage samples. We would also like to thank Dr. M. Yamanari and Professor Y. Yasuno at Tsukuba University for helpful advice and assistance in building and developing the PS-OCT system. This study was funded by EPSRC grant EP/F020422.

Reference

1. P. H. Tomlins and R. K. Wang, "Theory, developments, and applications of optical coherence tomography," *J. Phys. D* **38**(15), 2519–2535 (2005).
2. T. Xie, Y. Xia, S. Guo, P. Hoover, Z. Chen, and G. M. Peavy, "Topographical variations in the polarization sensitivity of articular cartilage as determined by polarization-sensitive optical coherence tomography and polarized light microscopy," *J. Biomed. Opt.* **13**(5), 054034 (2008).
3. N. Ugryumova, S. V. Gangnus, and S. J. Matcher, "Three-dimensional optic axis determination using variable-incidence-angle polarization-optical coherence tomography," *Opt. Lett.* **31**(15), 2305–2307 (2006).
4. F. Fanjul-Vélez and J. L. Arce-Diego, "Polarimetry of birefringent biological tissues with arbitrary fibril orientation and variable incidence angle," *Opt. Lett.* **35**(8), 1163–1165 (2010).
5. P. E. Andersen, L. Thrane, H. T. Yura, A. Tycho, T. M. Jorgensen, and M. H. Frosz, "Advanced modelling of optical coherence tomography systems," *Phys. Med. Biol.* **49**(7), 1307–1327 (2004).
6. V. V. Tuchin, L. V. Wang, and D. A. Zimnyakov, *Optical Polarization in Biomedical Optics*, Springer-Verlag, Berlin Heidelberg (2006).
7. A. Wax, C. Yang, M. G. Muller, R. Nines, C. W. Boone, V. E. Steele, G. D. Stoner, R. R. Dasari, and M. S. Feld, "In situ detection of neoplastic transformation and chemopreventive effects in rat esophagus epithelium using angle-resolved low-coherence interferometry," *Cancer Res.* **63**(13), 3556–3559 (2003).
8. V. C. Mow and A. Ratcliffe, "Structure and Function of Articular Cartilage and Meniscus," Chapter 4 in *Basic Orthopaedic Biomechanics*, V. C. Mow and W. C. Hayes, Eds., pp. 113–177, Lippincott-Raven, New York (1997).
9. Z. Lu, D. K. Kasaragod, and S. J. Matcher, "Optic axis determination by fibre-based polarization-sensitive swept-source optical coherence tomography," *Phys. Med. Biol.* **56**(4), 1105–1122 (2011).
10. P. H. Tomlins, O. Adegun, E. Hagi-Pavli, K. Piper, D. Bader, and F. Fortune, "Scattering attenuation microscopy of oral epithelial dysplasia," *J. Biomed. Opt.* **15**(6), 066003 (2010).
11. C. F. Bohren and D. R. Huffman, "Rayleigh-Gans Theory," Chapter 6 in *Absorption and Scattering of Light By Small Particles*, pp. 158–165, Wiley, New York (1983).
12. I. Freund, M. Deutsch, and A. Sprecher, "Connective tissue polarity. Optical second-harmonic microscopy, crossed-beam summation, and small-angle scattering in rat-tail tendon," *Biophys. J.* **50**(4), 693–712 (1986).